Optical-Absorption Edge and Raman Scattering in Ge_xSe_{1-x} Glasses

P. Tronc, M. Bensoussan, and A. Brenac
Centre National d'Etudes des Télécommunications, 196 rue de Paris, 92220 Bagneux, France

C. Sebenne
Laboratoire de Physique des Solides associé au Centre National de la Recherche Scientifique, Université de Paris VI, Paris, France

(Received 9 April 1973)

Optical-absorption-edge measurements and Raman scattering experiments on Ge_xSe_{1-x} glasses are reported for the range $0 \leq x \leq 0.4$. The change in the magnitude of the main peaks of Raman spectra (localized about 195, 215, and 250 cm^{-1}) and the variation of the optical-absorption edge as a function of x lead to a model of local structure for $x \leq 1/3$. In this range of concentrations, germanium atoms are coordinated with four selenium atoms. There is no Ge-Ge bond, and furthermore, Ge-Se-Ge sequences remain scarce as long as the germanium concentration of the mixture makes it possible.

I. INTRODUCTION

The interest of dealing with a binary system is to supply a parameter x (atomic percentage of germanium) that one can vary continuously, leading to different measurable effects. From this point of view, the Ge-Se system is very attractive, since it allows the formation of glasses in the range $x = 0$ to about $x = 0.42$. Furthermore the variation of x induces significant changes in the optical properties related to the electronic structure, as well as changes in the Raman spectrum related to the local atomic structure.

Optical-absorption-edge curves of Ge_xSe_{1-x} glasses and their Raman scattering spectra for a large number of x values are presented hereafter. To the best of our knowledge, it is the first systematic study of the optical-absorption edge of an amorphous mixture. We develop a structural model for these glasses from our experimental results and their dependence upon x. This model is used to determine the coordination numbers of germanium and selenium atoms and to explain the chemical bonds existing in the Ge_xSe_{1-x} glasses.

The phase diagram of the Ge-Se system has been investigated by many authors.[1-5] We reproduce in Fig. 1 a phase diagram compiled from the most recent papers. There are several crystalline compounds in the Ge-Se system: first of all, the single elements selenium and germanium. Three crystalline selenium varieties are known.[6] The trigonal one, isomorphous to the tellurium crystal, is made up of helicoidal chains. The two monoclinic forms (α and β) are Se_8 ring shaped, similar to the S_8 sulfur rings; they differ from one another mainly by the stacking of the rings. The selenium coordination number always remains equal to two and the distance from an atom to its two first neighbors is hardly altered when passing from one variety to the other one. The other elementary crystal of the system is the well-known germanium crystal. Furthermore, there are two binary crystals: the germanium mono- and di-selenides.

The germanium monoselenide GeSe crystallizes in the orthorhombic system.[7] Its structure, of the distorted NaCl type, is characterized by the double layers normal to the c axis and recalls the arsenic structure. This grey metallic-looking single crystal is easily cleavable in a direction parallel to the double-layered plane. Each selenium atom has three Ge neighbors and vice versa.

The germanium diselenide ($GeSe_2$) structure has not been yet determined. We assume that it is made of tetrahedra with four selenium atoms at the corners and one germanium atom at the center,

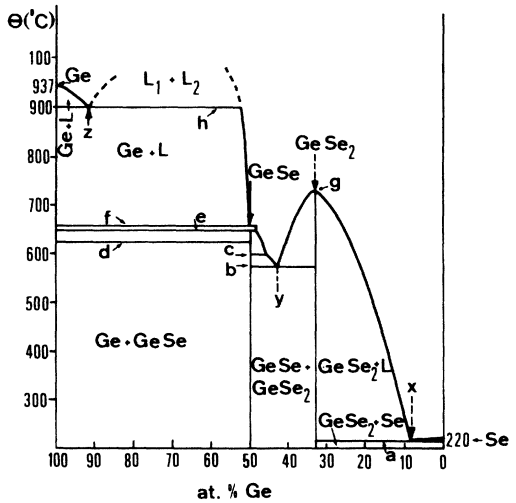

FIG. 1. Phase diagram of Ge-Se system. a: 218 °C (2); b: 580 °C (3), 578 °C (4), 573 °C (5); c: 630 °C (3), 603 °C (5); d: 627 °C (5); e: 660 °C (4), 651 °C (5); f: 666 °C (4), 661 °C (5); g: 740 °C (3, 4, 5); h: 900 °C (4), 890 °C (5); X: at.% Ge = 8 (2); Y: at.% Ge = 38 (3), 40-42 (4), 43 (5); Z: at.% Ge = 88-89 (4), 86 (5); (2): Dembovsky *et al.*; (3): Vinogradova *et al.*; (4): Ross *et al.*; (5): Quenez *et al.*

each selenium atom being shared by two neighboring tetrahedra. This assumption is supported by the great similarity of the Ge-S and the Ge-Se systems; on another hand, GeS_2, the structure of which has been investigated,[8] actually presents this type of configuration with a distorted tetrahedron. $GeSe_2$ is a yellow transparent cleavable crystal. It may be prepared by the Bridgman method or by a liquid-encapsulated growth technique.[9]

The ability of obtaining glasses from germanium and selenium in the Se-rich part of the diagram has been reported.[10–17] We succeeded in preparing glasses in the whole range $0 \leq x \leq 0.42$, and consequently for the $GeSe_2$ composition. These glasses exhibit no x-ray diffraction lines. The thin platelets (a few hundred microns), the composition of which is close to $GeSe_2$, appear dark red when looked through.

The properties of selenium in the field of optics and lattice vibrations have been dealt with in many papers: for example, the optical-absorption edge and the reflectivity of trigonal,[18] monoclinic,[19–21] and amorphous[22,23] selenium; Raman scattering in trigonal, α-monoclinic, and amorphous selenium,[24] and also infrared transmission.[25] By contrast, the properties of the vitreous and crystalline GeSe compounds are not so well known. Some papers about crystalline GeSe (electrical properties,[26] optical-absorption-edge measurements using nonpolarized light with an incidence normal to the cleavage plane and photoconductivity[27]) and about Ge_xSe_{1-x} glasses (electrical properties,[11,13–15] thermal conductivity,[28] infrared transmission[29]) may be quoted. The electrical resistivity of the glasses is always very high at room temperature (above 10^{12} Ω cm).

The structure of amorphous Ge_xSe_{1-x} films has been investigated by Fawcett *et al.*[30] using energy-filtered electron diffraction for the composition $x = 0$, $x = 0.32$, $x = 0.56$, and $x = 0.73$. They only considered the possibility of coordination numbers four and two for germanium and selenium, respectively, from $x = 0$ up to $x = 1$, even in the neighborhood of the GeSe composition; and they compared the mean coordination number per atom n_A measured in glasses to the values obtained with two theoretical models. In the first model, germanium and selenium atoms are coordinated completely at random ("random-covalent model"); in the other one, Ge-Ge bonds are forbidden ("chain-crossing model" only possible for $x \leq \frac{1}{3}$). For $x = 0.32$, the two theoretical values of n_A are equal and do not allow us to draw any conclusion about the existence of the Ge-Ge bonds. For $x = 0.56$, the random-covalent model does not seem to agree completely with measurements. For $x = 0.73$, the agreement is satisfactory.

II. PREPARATION AND CHARACTERIZATION OF MATERIALS

The starting materials are highly pure: intrinsic germanium with a 50-Ω cm resistivity (Vieille Montagne) and selenium 99.995% (Mining Chemical Products). The two elements are introduced in a quartz ampoule—internal diameter 17 mm—previously cleaned and outgased at 300 °C, then evacuated to 10^{-5} Torr and sealed. This ampoule, held in a rocking furnace, is rotated in an alternating way so that good homogenization can be obtained when the mixture has melted. After a 24-h plateau at a temperature between 700 and 900 °C according to the composition, the compound is cooled more or less rapidly, depending on the germanium concentration (quenching is necessary for the compounds near selenium and $GeSe_2$). The ingots are sliced, then mechanically polished to give samples with flat parallel faces, the thickness of which is between a few centimeters and 100 μm. With chemical thinning of polished 100-μm samples, the thickness can be reduced down to a few microns, while the surface quality remains good enough.

The uniformity of composition is tested by chemical analysis (colorimetry); the x variations so revealed in the ingots are less than 3% in relative value. These results are corroborated by the observation of the samples with the electron microprobe. Furthermore, the vitreous state of the material can be checked by the x-ray diffraction spectra, exhibiting no diffraction line. (The measurements are carried out with a powder goniometer Philips using the Cu $K\alpha_1$ radiation; the receptor is an amplitude-discriminating scintillator.)

On the other hand, the transmission-electron microscopy cannot be used, at least for Ge concentrations less than 25 at.%, because of the selenium sublimation under the action of the electron beam. For $x > 0.25$, the recrystallization of the compound into $GeSe_2$ disturbs the experiment.

The examination of carbon replicas by electron microscopy demonstrates the homogeneity of the compounds, in the limit of the resolution power (about 100 Å), except for very few bubbles with a diameter of about 1 μm that have been revealed by this type of analysis. An observation of the samples by infrared-transmission microscopy showed that the precipitates, reported by Vasko,[29] who assumes that they account for the crystalline $GeSe_2$ structure, are quite scarce and very small (about 10 μm).

The infrared-transmission study indicated that the absorption line near 750 cm^{-1} (probably due to oxygen) is extremely weak and that, as Vasko pointed out, the magnitude of the absorption line which appears at about 560 cm^{-1}, increases with the germanium concentration.

III. EXPERIMENTAL RESULTS

A. Raman Scattering

Generally, the absorption of the investigated Ge_xSe_{1-x} glasses is strong in the visible spectrum, which involves difficulties in obtaining Raman spectra. All the lasers classically used in the visible range are to be discarded, for the energy density that the sample can bear without being evaporated does not allow the disposal of an easily detectable signal.

The measurements we report in this paper have been carried out with the help of a 1.06-μm yttrium aluminum garnet laser with a power adapted to each sample but always near 1 W. The spectrometer was made by Coderg (PH-1 type). The detection is essentially made up of a S1-type cathode photomultiplier, cooled at about -70 °C. Taking account of the variation of the photomultiplier sensitivity versus frequency, on the one hand, and of the effect of Bose-Einstein statistics upon the line magnitudes on the other hand, the Stokes and anti-Stokes spectra supply rather equivalent information.

Figure 2 displays the whole of the significant experimental results, obtained from the anti-Stokes spectra, in the range 150–350 cm^{-1}. It is noticeable that a wide inelastic scattering band appears within the interval from 30 to 140 cm^{-1}, but its structure is not clear at all, and it seems hard at present to draw accurate information from it.

No quantitative comparison can be made between experiments because of fluctuations of laser-beam power and because of unavoidably irreproducible optical arrangements. However, some normalization being necessary, we took the 195-cm^{-1} line as a reference, and assigned to it an intensity proportional to the germanium concentration, for reasons that will appear clearer further on in the discussion. This line is only missing for the pure-selenium spectrum which was not normalized, but simply plotted using a coherent scale with the other spectra. Most of the spectra are the synthesis of many recordings made in similar experimental conditions, except for the 5-at.%-Ge sample, which could not be very accurately measured because of its great intolerance with regard to the laser beam; in this latter case, the comparison between the intensities of the lines at 195 and 250 cm^{-1} is more doubtful than for the other spectra.

The Raman spectrum of crystalline $GeSe_2$ was also achieved under classical experimental conditions with a krypton laser. These results, which will be the object of a further publication, show that a high-intensity peak exists at 213 cm^{-1}, and a weaker but significant one at 195 cm^{-1}.

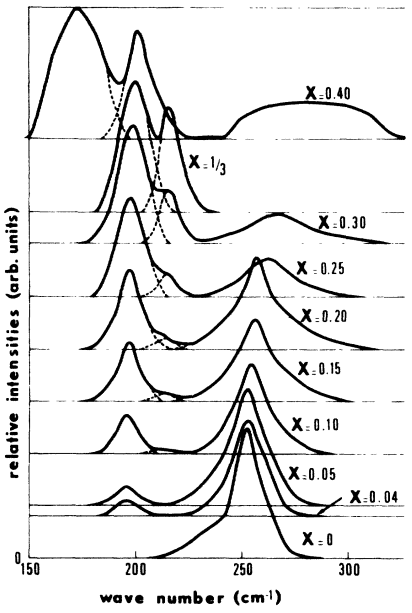

FIG. 2. Anti-Stokes Raman spectra of Ge_xSe_{1-x} glasses ($0 \leqslant x \leqslant 0.4$).

B. Optical-Absorption Edge

The measurements were performed with a HRS 1 Jobin-Yvon monochromator, fitted with 1220-lines/mm gratings. The output signal of the photomultiplier was detected with a lock-in amplifier.

All the absorption measurements (Fig. 3) have been performed at room temperature. The curves relative to trigonal selenium, α-monoclinic selenium, and crystalline GeSe, were drawn from Refs. 18, 21, and 27. We give our own results for crystalline $GeSe_2$ using nonpolarized light with an incidence normal to the cleavage plane (which includes two major crystalline axes). The absorption curves using polarized light have a few differences with the former curve, but these differences are small compared with those existing between this curve and the amorphous $GeSe_2$ curve.

When the germanium concentration increases from $x = 0$, the absorption curve begins to drift slowly towards the high energies; then shifting becomes more swift. At the same time, the slope of the curve decreases in a monotonic way, then does not vary any longer between $x = 0.3$ and $GeSe_2$. At last, the absorption is rapidly shifted towards the low energies, when x becomes larger than $\frac{1}{3}$.

In the range of the measured values of absorption coefficient α, three immediate conclusions may be drawn:

(i) For a given photon energy, the optical-absorption coefficient varies, in a monotonic way, versus x, between two definite compounds; it decreases from pure selenium to $GeSe_2$ and increases from $GeSe_2$ up to $x = 0.4$.

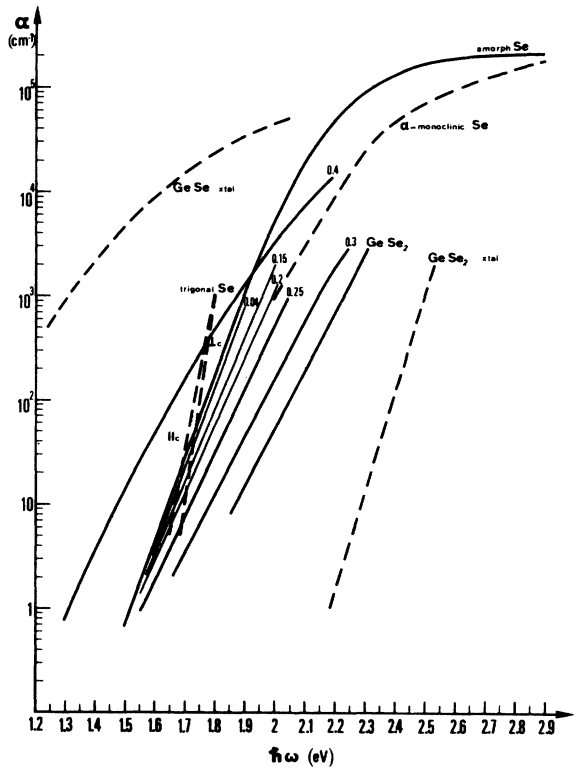

FIG. 3. Optical-absorption edges of Ge_xSe_{1-x} glasses.

(ii) For a given photon energy, the absorption coefficient is small for amorphous $GeSe_2$ compared to amorphous selenium (more precisely $\alpha_{GeSe_2} < 2 \times 10^{-2} \alpha_{Se}$).

(iii) The absorption curves of amorphous and crystalline $GeSe_2$ are much more different from one another (energy shift) than the curves of amorphous selenium from the curves of the crystalline selenium varieties.

IV. DISCUSSION

Figure 3 shows that the optical absorption of glasses with a germanium content inferior or equal to $GeSe_2$ composition ($x \leq \frac{1}{3}$)—to which this discussion will be limited—is lower than the optical absorption of amorphous selenium, for a given photon energy. The glass absorption is indeed very different from the pure-germanium absorption, which is yet high for photon energies near 1 eV.

When mixtures ($x \leq 0.42$) crystallize due to an intentionally slow cooling rate during preparation, the x-ray lines appearing are always characteristic of crystalline $GeSe_2$, except for glasses with very low germanium content (a few atomic percent) when selenium lines are seen; on the contrary, for $x \geq 0.43$, the quenched mixtures are always polycrystalline and all of them show the lines of crystalline GeSe. The tendency of glasses to reorganization is undoubtedly directed towards the crystalline structure of $GeSe_2$, except for compositions close to pure selenium; this prompts us to say that (i) the Ge-Ge bonds do not appreciably exist, and that (ii) the glass structure is locally similar either to pure crystalline selenium, or to crystalline $GeSe_2$, the amount of local $GeSe_2$-like centers obviously increasing with x.

These assumptions are supported by Raman measurements which indicate that the statement of basic differences in the nature of chemical bonds between glasses and crystals (e.g., coordination-number changes of Ge or Se) may be discarded; all the Raman lines of the glasses are indeed found again, either in the pure selenium or crystalline $GeSe_2$ spectrum (see below). We assumed that crystalline $GeSe_2$ was made of $GeSe_4$ tetrahedra; so, we allot the coordination numbers four and two, respectively to germanium and selenium in the glasses and, considering the above-mentioned reasons, we consequently leave aside coordination number three for both germanium and selenium, which would correspond to a local crystalline GeSe-like structure. We do not take into account here the unsatisfied valencies, because EPR investigations carried out on different chalcogenide glasses lead to assume their number to be negligible[31,32]; on another hand, the impossibility of substantially modifying conductivity of chalcogenides by doping is generally taken as a consequence of saturation of all valencies.

Detailed examination of the case relative to amorphous $GeSe_2$ provides a good illustration of the preceding considerations. For amorphous $GeSe_2$, a simple enumeration of bonds shows that the possible existence of Ge-Ge bonds would involve the existence of Se-Se bonds and reciprocally. Now, on one hand, the only x-ray lines after recrystallization are the crystalline $GeSe_2$ lines; on the other hand, the Raman scattering spectrum of this glass shows neither selenium nor germanium lines, and the only two existing lines are corresponding to frequencies of crystalline $GeSe_2$ (195 and 215 cm^{-1}).

For glasses with germanium content higher than $x = \frac{1}{3}$, the ability of two germanium atoms to coordinate, and/or the coordination-number change of germanium and selenium, i.e., the formation of crystalline GeSe-like local centers, must be taken into account. Our experimental results are yet too incomplete for $x > \frac{1}{3}$, to approach this problem.

A. The Model

The structural model we can develop from the preceding considerations is made of germanium atoms with coordination number four and selenium atoms with coordination number two. All valen-

cies are satisfied. Two germanium atoms cannot be bound together. This model can be used only in the range $0 \leq x \leq \frac{1}{3}$.

In our model, we exclude *a priori* any possibility of double bonds Ge-Se, which seems unlikely because of the tetrahedric structure of crystalline $GeSe_2$, as well as existence of Se_2 molecules. These molecules are surely scarce, if even they exist, in amorphous pure selenium (the lattice vibration characteristics of which, as pointed out by infrared absorption and by Raman scattering, directly derive from the trigonal and monoclinic selenium characteristics); on the other hand, we shall see that Raman measurements on the Ge_xSe_{1-x} glasses show that germanium atoms tend to be as diluted as possible: for composition $x = 0.2$, $GeSe_4$ groups are linked together by Se-Se bonds, no atom remaining available to form Se_2 molecules.

We can finally note that the germanium and selenium atomic masses are close together (respectively, 72.6 and 78.96) and that the density of glasses undergoes very little variation between $x = 0$ and $x = 0.4$. In order to make our further calculations simpler, we may assume that one atom either of germanium or of selenium takes up equal and constant volumes in the glasses, whatever x may be.

B. Raman Scattering

The spectra that can be seen in Fig. 2 show three lines located at about 195, 215, and 250 cm^{-1}. The line at 195 cm^{-1}, also appearing in crystalline $GeSe_2$, becomes visible as soon as germanium is introduced, even in low concentration. It strongly increases with germanium content and still persists beyond $GeSe_2$ composition; it is clear that this line is characteristic of the existence of germanium in the selenium environment.

The line at 215 cm^{-1}, very close to the one at 213 cm^{-1}, existing in crystalline $GeSe_2$ appears much more slowly than the previous one as germanium concentration increases; it goes up to an intensity that can be compared to that of $GeSe_2$, and then completely disappears for the 40-at.%-Ge glass. We assume it has its origin in the sequence of three atoms: Ge-Se-Ge.

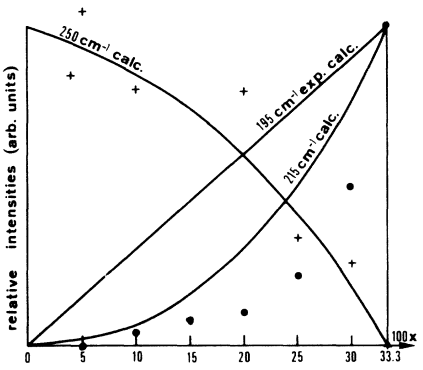

FIG. 4. Raman lines intensities (1st model). •: 215 cm^{-1} (expt.); +: 250 cm^{-1} (expt.).

It is to be noted that the relative position of Raman lines at 195 and 215 cm^{-1} in an energy scale, agrees well with what is suggested by the atomic-masses ratio of selenium and germanium.

The line located around 250 cm^{-1}, which is the only one appearing in pure selenium, may be considered, from the outset, as connected with the Se-Se bond. It has already been obtained by other researchers on amorphous selenium and different crystalline varieties.[24]

The shoulder located at about 230 cm^{-1} vanishes as soon as the glass content gets over 4 at.% of Ge. From relevant literature, the 250-cm^{-1} peak is characteristic of Se_8-ring-shaped selenium and the 230-cm^{-1} peak of the chainlike selenium. It can be thought that a local configuration of the selenium atoms, similar to monoclinic selenium, is favored by the introduction of germanium. Due to experimental sensitivity, this line is completely removed for $GeSe_2$ composition. The line that can be seen around 300 cm^{-1} for $x = 0.4$ looks very different, and seems to have another origin than the Se-Se bond. However, if the line located at 250 cm^{-1} was strictly characteristic of the Se-Se bond, its intensity would be proportional to the number of these bonds, which—as we show further on—varies as $(1 - 3x)$ as a function of x. Now, Fig. 4 shows that this intensity is higher than that given by such a dependence on x. Besides, it seems right to admit that the vibration modes of a selenium atom bound to a selenium atom, on one side, and to a germanium atom, on the other side, are not much different from the modes of such a selenium bound to two selenium atoms; the germanium atomic mass is indeed not much different from that of the selenium, and furthermore, the above-mentioned selenium atom is always included in a linear structure which differs little from the one found in pure selenium. So, we admit that the vibration modes of all selenium atoms not bound to two germanium atoms are characterized by the lines located at 250 cm^{-1}. This also explains why the line shifts towards the high energies and broadens for increasing values of x.

Now, we are going to check the coordination numbers two and four, respectively, allotted to selenium and germanium, as well as the nonexistence of the Ge-Ge bond for $x \leq \frac{1}{3}$, by calculating the intensity variations of the three Raman lines, from the structural model. So, the assignment of the lines will be *"a posteriori"* justified by the agreement between calculation and measurements. We assume that the lattice-vibration frequencies only depend on the nature of atoms (germanium

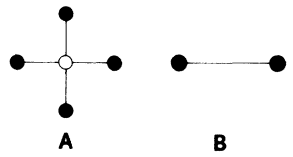

FIG. 5. Elements A and B.

or selenium) and on their first neighbors.

In our lattice model, the four allowed sequences of three atoms are as follows: Se-Ge-Se, Ge-Se-Se, Ge-Se-Ge, Se-Se-Se.

In order to make counting easier, it is convenient to consider the lattice as constituted of the following two elements (Fig. 5): element A—a germanium atom bound to four selenium atoms; element B—two selenium atoms bound together, each selenium atom being shared by neighboring elements. The structure of elements A and B precludes the opportunity of coordinating two germanium atoms together and there is a one-to-one correspondence between the four above-enumerated sequences and the elements A and the bonds AB, AA, and BB respectively. Assuming that germanium and selenium atoms take up the same volume, the number of elements A per unit is varying as x, the number of elements B as $(1-3x)$.

Statistical calculation made in Appendix A by assuming that all configurations of the lattice AB are equiprobable (provided that valencies are satisfied) shows that the number of each of the four sequences, respectively, varies vs x, as x, $x(1-3x)/(1-x)$, $x^2/(1-x)$, and $(1-3x)^2/(1-x)$. The number of Se-Se bonds is equal to the number of elements B.

If our model is valid, the areas below the peaks at 195, 215, and 250 cm^{-1} should vary vs x as x, $x^2/(1-x)$, and $(1-3x)(1+x)/(1-x)$, respectively. In Fig. 4, we plotted the theoretical curves and the experimental points. By normalizing as we did for the Raman spectra, the agreement is automatically perfect for the 195-cm^{-1} line. For the two other lines, it may be seen that the experimental variations are slower than it would be prescribed by the model for $x \leq 0.2$, and then faster. This phenomenon may be interpreted by admitting the fact that germanium atoms tend to be diluted in selenium: two germanium atoms avoid to be bound to the same selenium atom as far as germanium content makes it possible. The new model that can be derived for $x \leq 0.2$ is made of the following two elements: element A—as defined above; element C—one selenium atom, no selenium atom being shared by neighboring elements.

In this new model, the line at 250 cm^{-1} varies as $(1-x)$ up to $x=0.2$. For $x>0.2$, the number of selenium atoms not bound to two germanium atoms linearly decreases with x and becomes null for $x=\frac{1}{3}$. The line intensity at 215 cm^{-1} is zero up to $x=0.2$ and then linearly increases with x. This new model yet entails some discrepancies with respect to measurements; the most significant difference is the experimental emergence of the 215-cm^{-1} line before $x=0.2$ (Fig. 6). The position of the corresponding experimental points—situated between the curves derived from the two models—suggests that the glass structure is, in fact, intermediate between the two theoretical descriptions. It is also likely that the existence of the line at 215 cm^{-1} for $x<0.2$ is partly due to local fluctuations of composition-inducing zones where germanium content is superior to 0.2.

C. Optical-Absorption Edge

The interpretation of the experimental results will also be attempted only for compositions between pure selenium and $GeSe_2$. It is known that there can be only two kinds of bonds: Ge-Se and Se-Se (the first considered being the bond existing in crystalline $GeSe_2$). Then, we assume that α_x, optical-absorption coefficient of the compounds, is the sum of a seleniumlike absorption term and of a $GeSe_2$-like term, respective weights of these two terms being proportional to the number of bonds of each type. Therefore, from the optical-absorption point of view, with our model we can consider the glassy platelet as the superposition of a pure amorphous selenium platelet and of a pure amorphous $GeSe_2$ platelet. Counting the number of bonds of each type and assuming that volumes occupied by a selenium and a germanium atom are equal, we can expand the formula giving the absorption coefficient α_x vs the coefficient α_{Se} of pure amorphous selenium and α_{GeSe_2} of amorphous $GeSe_2$, for a given photon energy:

$$\alpha_x=(1-3x)\alpha_{Se}+3x\alpha_{GeSe_2},\quad 0\leq x\leq \tfrac{1}{3}. \tag{1}$$

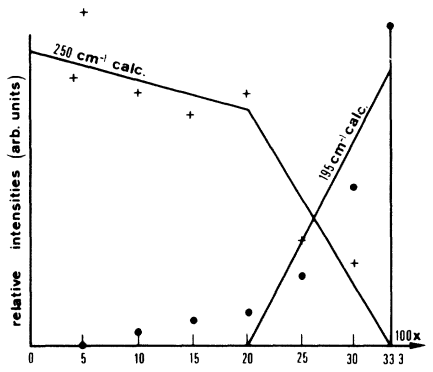

FIG. 6. Raman lines intensities (2nd model). •: 215 cm^{-1} (expt.); +: 250 cm^{-1} (expt.).

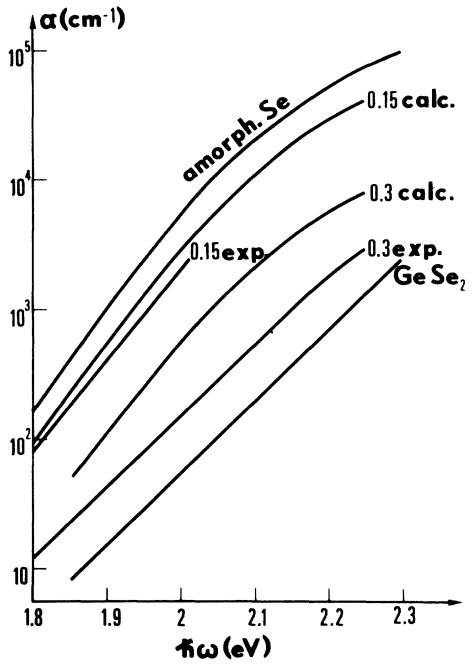

FIG. 7. Optical-absorption edges of Ge_xSe_{1-x} glasses ($0 \leq x \leq \frac{1}{3}$, 1st model).

α_{GeSe_2} is always very small compared to α_{Se}, in the whole energy range where these coefficients were simultaneously measured ($\alpha_{GeSe_2}/\alpha_{Se} < 2\times10^{-2}$).

Formula (1) may then be developed as below:

$$\log_{10}\alpha_x = \log_{10}\alpha_{Se} + \log_{10}(1-3x) + \frac{1.3x}{1-3x}\,\frac{\alpha_{GeSe_2}}{\alpha_{Se}}, \quad \text{for } x \leq 0.30. \quad (2)$$

The term $[1.3x/(1-3x)]\alpha_{GeSe_2}/\alpha_{Se}$ is negligible (less than 8×10^{-2} for $x = 0.3$).

Before comparing theoretical results with measurements, it is, besides, advisable to investigate the sensitivity of the model to composition variations. In Appendix B, we prove that local fluctuations of composition do not modify the value of α_x and that the mean deviation from the nominal composition is appreciable but for high germanium contents.

To make comparison easier, the results of theory and measurements have been plotted in Fig. 7, for the two compositions $x = 0.15$ and $x = 0.30$. The sense of α_x variation vs x is the same, but the amplitude of variation is underrated by theory, and difference is too high to be accounted for by a deviation from nominal composition. It is even more significant that the slope of the experimental absorption curve begins to decrease appreciably for $x = 0.15$, whereas it is predicted by theory to be rather constant and equal to the slope of selenium. (This results in the theory of the fact that absorption is always very small for amorphous $GeSe_2$ compared to selenium.)

The difference between the results provided by the model and the measurements can be ascribed first to the oversimplified assumption concerning optical-absorption mechanism. In fact, as is suggested by the tight-binding approach, it would be better that all first neighbors of each atom should be taken into account to determine the allowed energetic levels for valence and conduction electrons.[33-35]

In the absorption model presented above, the germanium atom has effectively the same first neighbors (four selenium atoms) as in $GeSe_2$, just as the selenium atom bound to two other selenium atoms has the same first neighbors as in pure selenium. On the contrary, nothing in the model is accounting for the energetic levels of the selenium atom bound to one selenium and one germanium atom. The number of selenium atoms of this kind is varying vs x as $x(1-3x)/(1-x)$; it becomes null for pure selenium and $GeSe_2$ and goes to a maximum for $x = 0.18$. It is shown by experimental curves that slope variation is the most important near $x = 0.20$.

To make this study complete, one must not forget that germanium atoms tend to be diluted in the lattice, as was brought to evidence by Raman scattering. We are therefore led to redefine our absorption model in the following way:

(a) In the interval $0 \leq x \leq 0.2$, the lattice is constituted from the elements A and C as defined above, no selenium atom being shared by neighboring elements. Absorption of the $GeSe_4$ compound ($x = 0.2$)—only made of elements A—and absorption of pure amorphous selenium—only made of elements C—being taken as references, we find the relation (3) by arguing in the same way as above:

$$\alpha_x = (1-5x)\alpha_{Se} + 5x\alpha_{GeSe_4}\ ; \quad (3)$$

but, in that case, each element C (selenium atom) has the same first neighbors as the selenium atom in pure selenium and each element A has the same first neighbors (four selenium atoms) as in pure $GeSe_4$. All the first neighbors of each atom were consequently taken into account for determination of its absorption. The linearity of formula (3) vs x cancels the effect of local fluctuations of composition on absorption.

Figure 8 shows that agreement between the model and measurements is excellent (it will be noted that, in the model relative to $GeSe_4$ composition, each selenium atom is coordinated to one germanium atom and to another selenium atom).

(b) In the interval $0.2 \leq x \leq 0.33$, the lattice is constituted by the following two elements (Fig. 9): element D—two germanium atoms bound through two selenium atoms; element E—two germanium

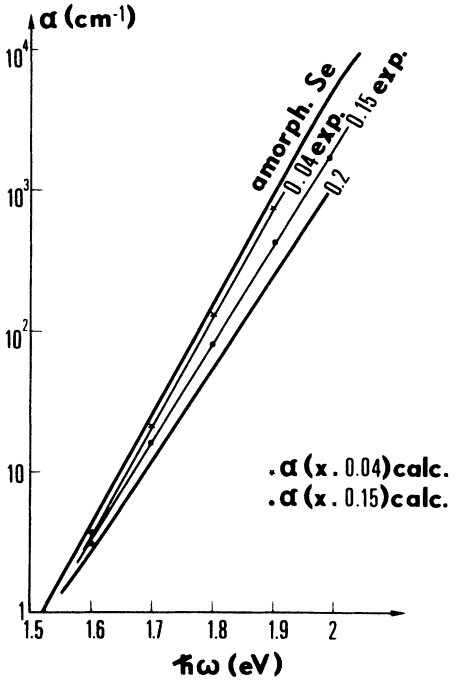

FIG. 8. Optical-absorption edges of Ge_xSe_{1-x} glasses ($0 \leqslant x \leqslant 0.2$, 2nd model).

atoms bound through one selenium atom, each germanium atom being shared by neighboring elements. D and E are the constitutive elements of the $GeSe_4$ and $GeSe_2$ compounds. In a similar manner, we can write

$$\alpha_x = \tfrac{5}{2}(1-3x)\alpha_{GeSe_4} + \tfrac{3}{2}(5x-1)\alpha_{GeSe_2} . \quad (4)$$

Again, at least the first neighbors of each atom are taken into account to determine absorption. However, agreement with measurements is not thoroughly satisfactory: the amplitude of variations vs x is yet underrated by the model (Fig. 10).

This disagreement may be ascribed to a tendency to order, which appears in glasses, the germanium content of which is above $x = 0.2$. (Indeed, it is precisely for these glasses that the melt must be rapidly quenched during a preparation in order to avoid recrystallization, the necessary quenching rate rising to a maximum for $GeSe_2$ composition.) It can be seen moreover that the absorption coefficient is much smaller still when the solid is completely ordered (crystalline $GeSe_2$),

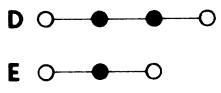

FIG. 9. Elements D and E.

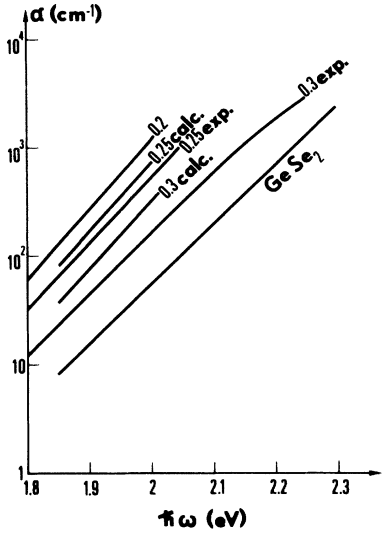

FIG. 10. Optical-absorption edges of Ge_xSe_{1-x} glasses ($0.2 \leqslant x \leqslant \frac{1}{3}$, 2nd model).

for a given photon energy.

Nevertheless, disorder seems to remain high for amorphous $GeSe_2$ and neighboring compositions. This point is, in fact, suggested by two experimental results: (i) The optical-absorption-edge curves measured at liquid-nitrogen temperature for $x = 0.3$ and $x = \frac{1}{3}$ keep parallel to the corresponding curves measured at room temperature (the slope of the optical-absorption-edge curves would be due to disorder rather than to electron-phonon interactions, for instance). (ii) The important energy shift between the optical-absorption-edge curves of amorphous $GeSe_2$ and crystalline $GeSe_2$.

We believe that this disagreement for $x > 0.2$ emphasizes the limits of validity of our model. The latter looks, indeed, well adapted to a statistical description of the nature of bonds existing in the amorphous binary lattice but, on the other hand, it gives no idea of possible stacking modes of elementary cells, such as $GeSe_4$ tetrahedra (elements A). These elementary cells are likely to be responsible for tendency to order (contrary to linear selenium chains) because of the bonds of germanium.

Concerning the absorption curve of the $Ge_{0.4}Se_{0.6}$ glass, its localization between amorphous $GeSe_2$ and crystalline $GeSe_2$, and the fact that it is not rectilinear, are prompting us to an interpolation between $GeSe_2$ and GeSe. We did not approach these calculations. Several curves will have to be recorded for compositions between $x = \frac{1}{3}$ and $x = \frac{1}{2}$. Investigation on the topological model of selenium and germanium coordination-number changes, respectively, from two and four to three seems rather complicated. We checked that the absorption curve

is shifted, keeping appreciably parallel to itself, between 300 and 95 °K for $x = 0.4$.

V. CONCLUSION

A structural model for the Ge_xSe_{1-x} glasses has been proposed for $x \leq \frac{1}{3}$ from the Raman spectra and the optical-absorption edges. This model, corroborated by the x-ray investigation of recrystallized samples, is formed by germanium atoms of coordination four and selenium atoms of coordination two, the Ge-Ge bonds being statistically forbidden. Moreover, the germanium atoms tend to part one from the others as far as germanium content of the mixture allows.

This shows how interesting it is to get use of glasses distributed in a wide composition range. It is possible, indeed, to determine the origin of the observed Raman peaks and the optical-absorption mechanism without ambiguity from their variations as a function of x.

The results here obtained raise some interesting questions; for instance, the variations of the slope and of the localization of optical-absorption-edge curve vs x, as well as the great difference between amorphous and crystalline $GeSe_2$, call for a careful study of the Ge-Se bond. Investigation of glasses for $\frac{1}{3} \leq x \leq \frac{1}{2}$, i.e., between $GeSe_2$ and GeSe, which both exist in the crystalline state, would be another interesting subject.

ACKNOWLEDGMENTS

. It is a pleasure to thank J. Theodore and the CCM Department in the Centre National d'Etudes des Télécommunications, who contributed to the preparation of our samples and performed the characterization tests, and more especially J. Burgeat and G. Le Roux, who carried out the x-ray measurements, and A. M. Pougnet, who was in charge of the chemical analysis. We are indebted to R. Beserman, J. F. Morhange, and C. Julien, who made their Raman equipment available to us.

APPENDIX A

The coordination numbers of elements A and B are, respectively, four and two. It is assumed that each valency of an element-B, for example—is connected with a definite type of element A or B, in a statistical proportion of cases equal to the proportion of valencies to be satisfied relative to this type of elements in the lattice. N being the total number of atoms, the number of elements A is Nx, the number of elements B is $N(1-3x)$. The number of valencies to be satisfied are, respectively, $4Nx$ and $2N(1-3x)$. Each valency of an element B is therefore connected with an element A or B in a statistical proportion of cases respectively equal to $p_{AB} = 2x/(1-x)$ and $p_{BB} = (1-3x)/(1-x)$. The number of bonds AB, for instance, is equal to the number of elements B multiplied by p_{AB}, i.e., $[2x(1-3x)/1-x]N$. (Each element B has two valencies, but each bond with another element is obviously attributed only for the half to that element.)

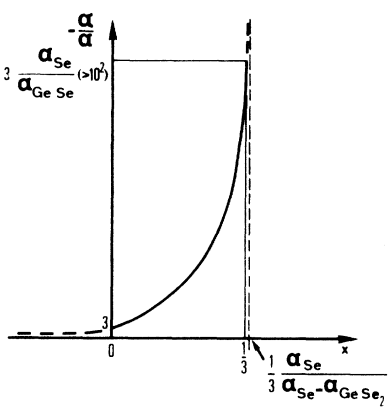

FIG. 11. Sensitivity of the first model to an uniform deviation from the nominal composition.

APPENDIX B

In Fig. 11, the logarithmic derivative of α_x with respect to x is plotted vs x. In the model, it is an expression of the sensitivity of α_x to a fixed and uniform deviation from the nominal composition. This sensitivity increases as one gets closer to $GeSe_2$ (the logarithmic derivative is superior to 10^2 for composition close to $GeSe_2$).

On the contrary, a Gaussian distribution of the variation with respect to an average composition x_0 is introducing no error upon the value of α_{x_0}. The transmitted energy for a sample with a thickness d is actually proportional to $\exp[-\sum(\alpha_{x_0+\Delta x}\Delta d)]$ (no account being taken of the variation of the reflexion coefficient due to fluctuations around x_0): to each elementary step Δd is corresponding another step, of same length, for which the variation is $-\Delta x$, and these two effects cancel each other because of linear dependence of α_x on x. This would be also true for any variation distribution law symmetrical around x_0. The only compositions for which this argument is not valid are those very close to $GeSe_2$, because α_x is certainly passing through a minimum for $x = \frac{1}{3}$ (as suggested by the measurements for $x = 0.4$). A composition variation around $GeSe_2$ always implies an increase of the measured absorption coefficient. The measured value of α_{GeSe_2} is therefore always at least equal to the actual value.

[1]Liu Ch'un-hua, A. S. Pashinkin, and A. V. Novoselova, Dokl. Akad. Nauk SSSR **146**, 1092 (1962).
[2]S. A. Dembovskii, G. Z. Vinogradova, and A. S. Pashinkin, Russ. J. Inorg. Chem. **10**, 903 (1963).
[3]C. Z. Vinogradova, S. A. Dembovskii, and N. B. Sivkova, Russ. J. Inorg. Chem. **13**, 1051 (1968).
[4]L. Ross and M. Bourgon, Can. J. Chem. **47**, 2555 (1969).
[5]P. Quenez, P. Khodadad, and R. Ceolin, Bull. Soc. Chim. Fr. **1**, 117 (1972).
[6]P. Unger and P. Cherin, in *The Physics of Selenium and Tellurium*, edited by W. C. Cooper (Pergamon, Oxford, England, 1969), p. 223.
[7]A. Okazaki, J. Phys. Soc. Jap. **13**, 1151 (1958).
[8]Liu Ch'un-hua *et al.*, Proc. Acad. Sci. USSR Phys. Chem. Sect. **151**, 662 (1963).
[9]M. Bensoussan, A. Brenac, J. Thomas, and P. Tronc, J. Cryst. Growth **15**, 79 (1972).
[10]S. V. Nemilov, Zh. Prikl. Khim. **37**, 1020 (1964).
[11]Z. U. Borisova, R. L. Myuller, and Chin Cheng Ts'ai, Zh. Prikl. Khim. **35**, 774 (1962).
[12]Z. U. Borisova and A. V. Pazin, in *Solid State Chemistry*, edited by Z. U. Borisova (Consultants Bureau, New York, 1966), p. 63.
[13]L. A. Baidakov, in Ref. 12, p. 164.
[14]Z. U. Borisova, E. R. Shokol'nikov, and I. I. Kozhima, in Ref. 12, p. 164.
[15]A. Feltz, H. J. Büttner, F. J. Lippmann, and W. Maul, J. Non-Cryst. Solids **8–10**, 64 (1972).
[16]R. E. Loehman, A. J. Armstrong, D. W. Firestone, and R. W. Gould, J. Non-Cryst. Solids **8–10**, 72 (1972).
[17]R. W. Haisty and H. Krebs, in Ref. 6, p. 345.
[18]W. Henrion, in Ref. 6, p. 75.
[19]G. B. Abdullayev, Y. G. Asadov, and K. P. Mamedov, in Ref. 6, p. 179.
[20]A. G. Leiga, J. Opt. Soc. Am. **58**, 1441 (1968).
[21]J. C. Knights and E. A. Davis, Solid State Commun. **11**, 543 (1972).
[22]J. L. Hartke and P. Regensburger, Phys. Rev. **139**, A970 (1965).
[23]G. Weiser and J. Stuke, Phys. Status Solidi **35**, 747 (1969).
[24]A. Mooradian and G. B. Wright, in Ref. 6, p. 269.
[25]G. Lukovsky, in Ref. 6, p. 255.
[26]B. Asanabe and A. Okazaki, J. Phys. Soc. Jap. **15**, 989 (1960).
[27]C. R. Kannewurf and R. J. Cashman, J. Phys. Chem. Solids **22**, 293 (1961).
[28]A. S. Okhotin, A. M. Krestovnikov, A. A. Aivazov, and A. S. Pushkarskii, Phys. Status Solidi **31**, 485 (1969).
[29]A. Vasko, in Ref. 6, p. 241.
[30]R. W. Fawcett, C. N. J. Wagner, and G. S. Cargill, III, J. Non-Cryst. Solids **8–10**, 369 (1972).
[31]S. C. Agarwal and H. Fritzsche, Bull. Am. Phys. Soc. **15**, 244 (1970).
[32]H. Fritzsche, J. Non-Cryst. Solids **6**, 49 (1971).
[33]D. Weaire and M. F. Thorpe, Phys. Rev. B **4**, 2508 (1971).
[34]D. Weaire and M. F. Thorpe, Phys. Rev. B **4**, 3517 (1971).
[35]M. F. Thorpe, D. Weaire, and R. Alben, Phys. Rev. B 7, 3777 (1973).